Electronic Supplementary Material (ESI) for Sustainable Energy & Fuels.

Supporting Information

MOF-derived C@NiO@Ni electrocatalyst for N_2 conversion to NH_3 in alkaline electrolytes

Shijian Luo, Xiaoman Li*, Wanguo Gao, Haiqiang Zhang and Min Luo*

State Key Laboratory of High-efficiency Utilization of Coal and Green Chemical Engineering，School of Chemistry and Chemical Engineering, Ningxia University, Yinchuan, Ningxia, 750021, P.R.China

**Corresponding author: Min Luo martinluomin@163.com，*
Xiaoman Li lixm2017@nxu.edu.cn

Content

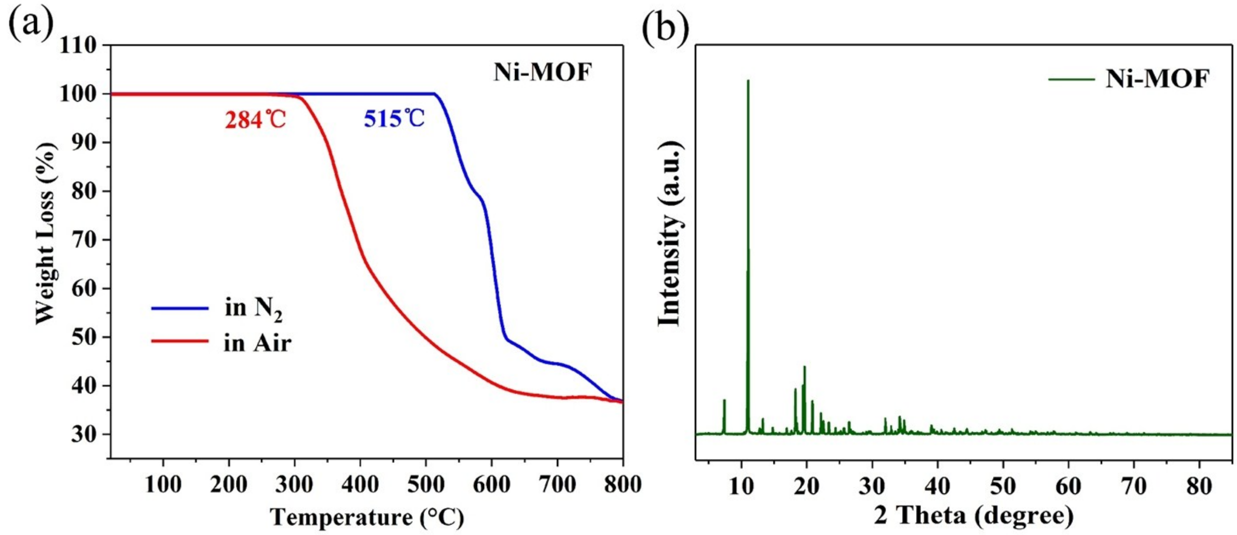

Fig. S1. (a) Thermogravimetric curve of Ni-MOF (Ni-BTC) in Air and N_2. (b) XRD pattern of Ni-MOF (Ni-BTC).

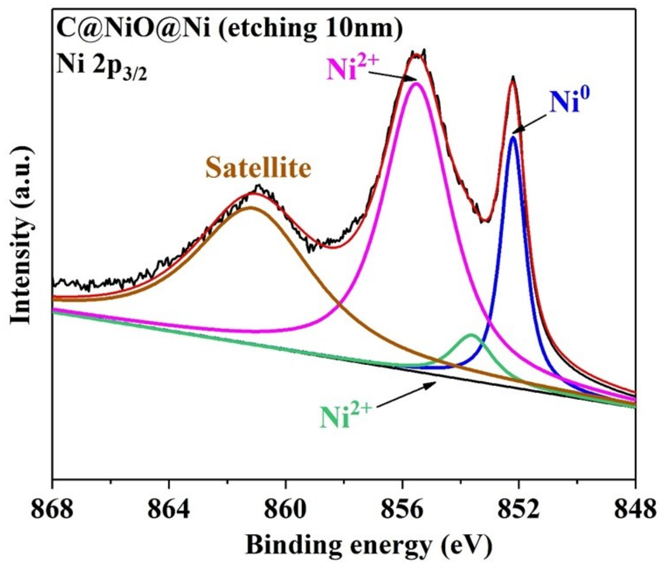

Fig. S2. The Ni $2p_{3/2}$ XPS pattern using Ar particles to etch C@NiO@Ni for 10 nm.

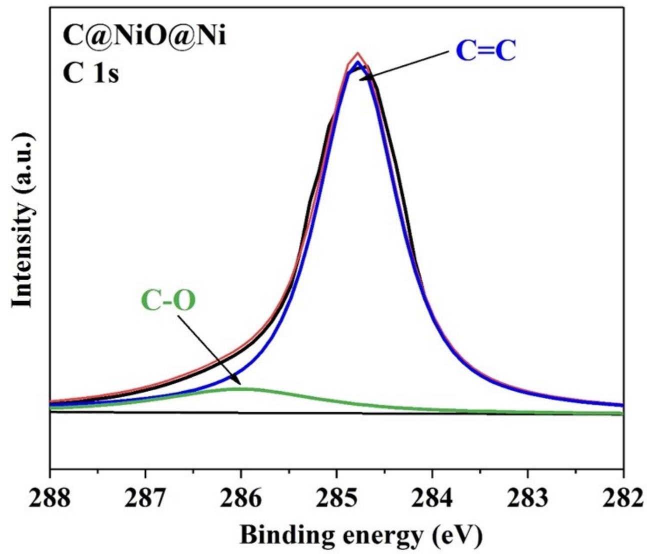

Fig. S3. XPS C 1s spectra for the C@NiO@Ni.

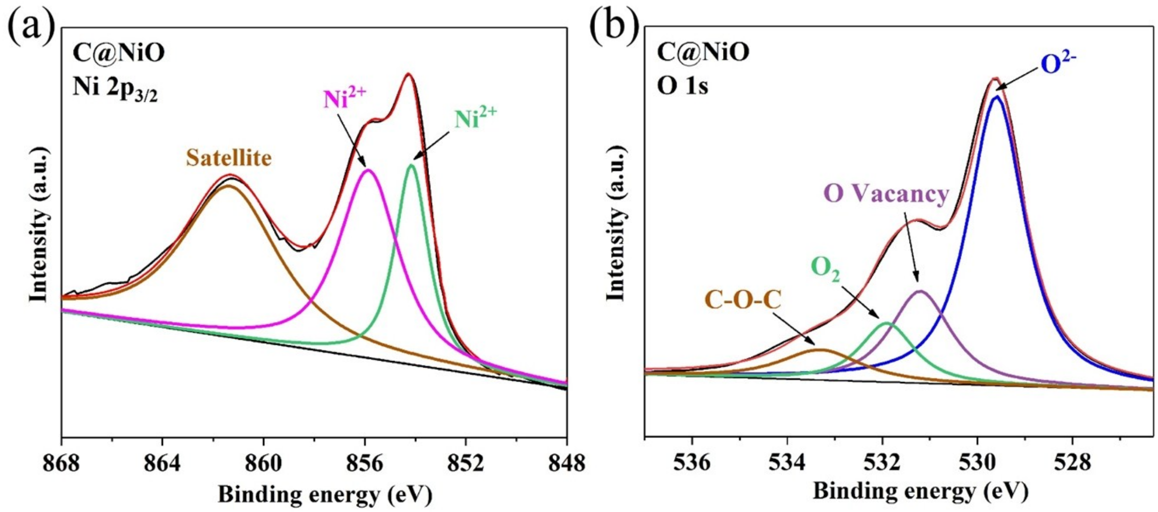

Fig. S4. XPS Ni $2p_{3/2}$ (a) and O 1s (b) spectra for the C@NiO.

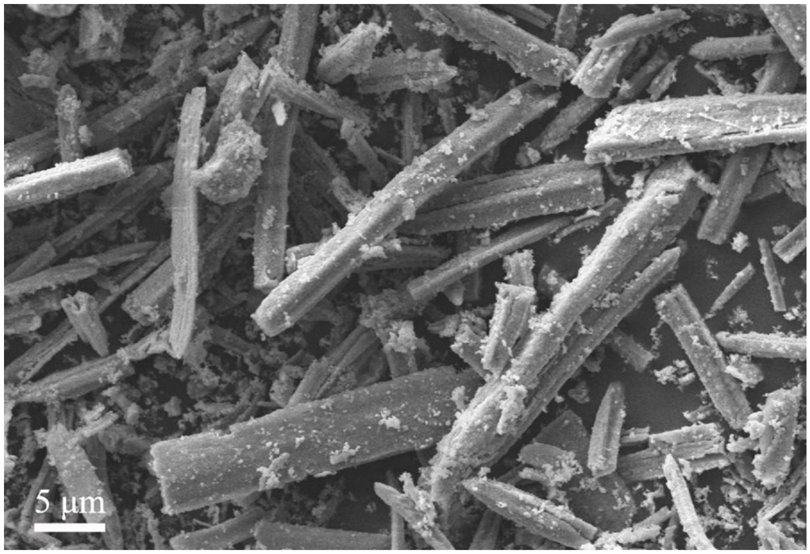

Fig. S5. SEM image of Ni-MOF (Ni-BTC) precursor.

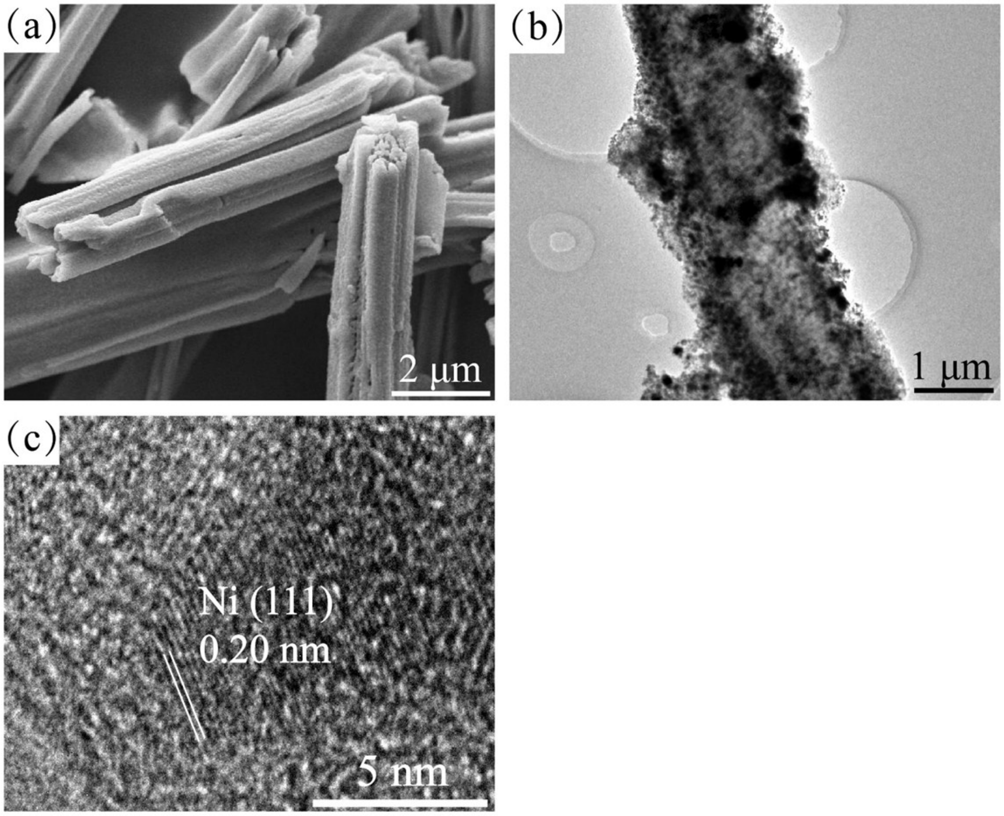

Fig. S6. (a) SEM image, (b) TEM image and (c) HRTEM image of C@Ni microtubes.

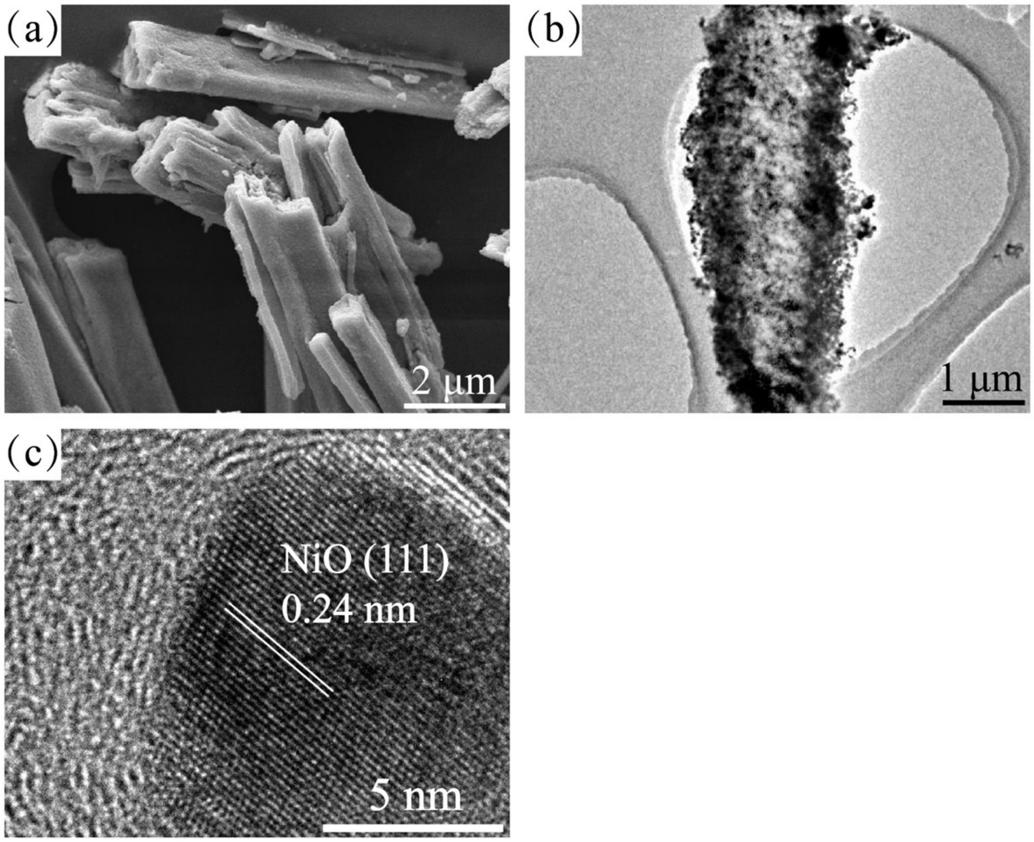

Fig. S7. (a) SEM image, (b) TEM image and (c) HRTEM image of C@NiO microtubes.

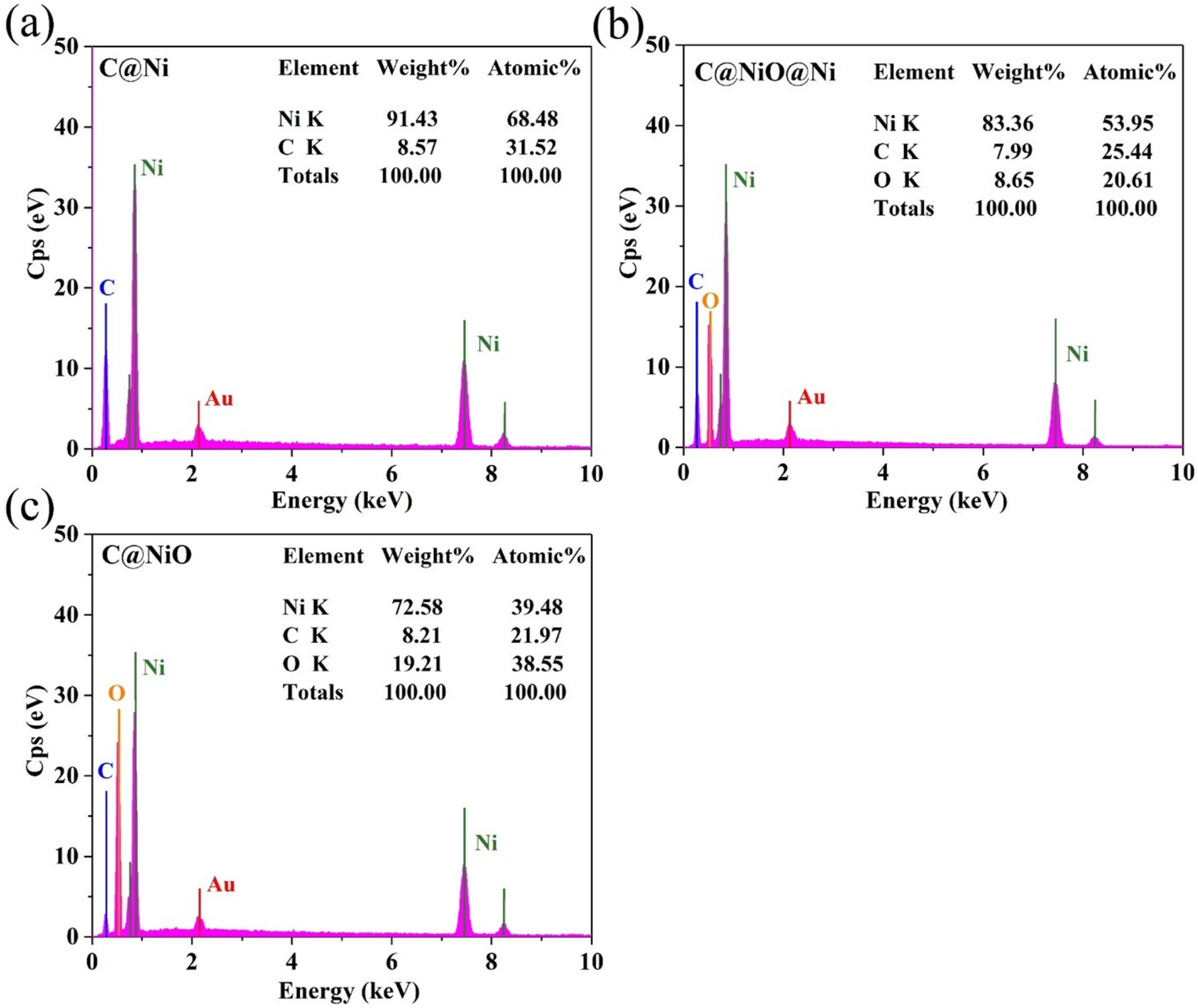

Fig. S8. (a) EDX of C@Ni. (b) EDX of C@NiO@Ni. (c) EDX of C@NiO.

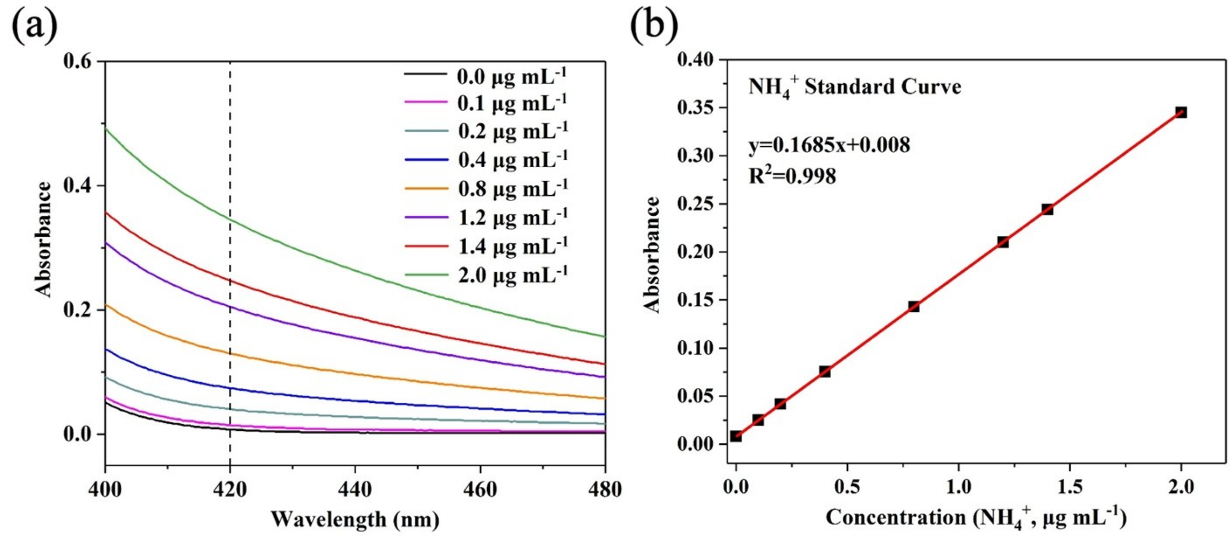

Fig. S9. (a) UV-Vis absorption curves of Nessler's reagent assays kept with different concentrations of NH_4^+ ions. (b) A calibration curve used to estimate the concentrations of NH_4^+ ions.

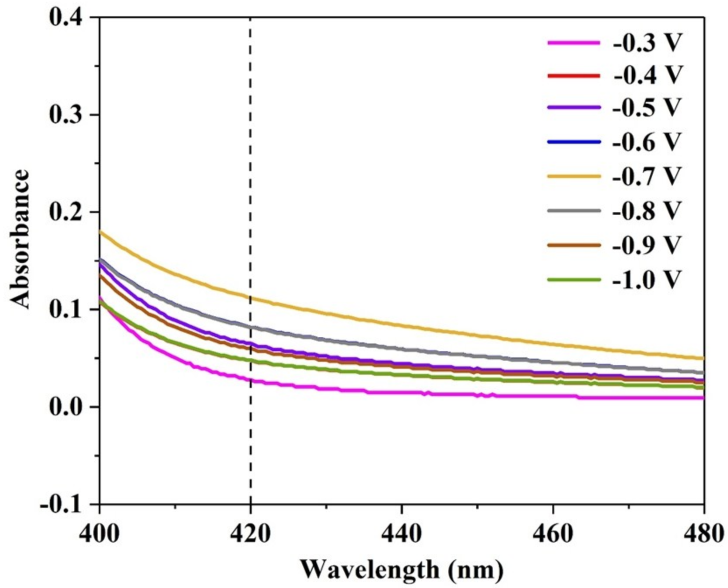

Fig. S10. UV-Vis absorption curves of the electrolyte after tests of C@NiO@Ni at different potentials.

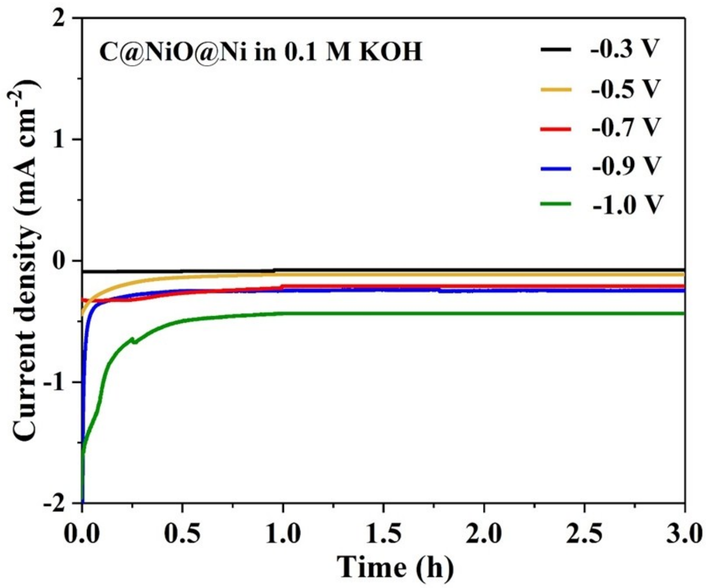

Fig. S11. Chronoamperometry results of C@NiO@Ni at the corresponding potentials.

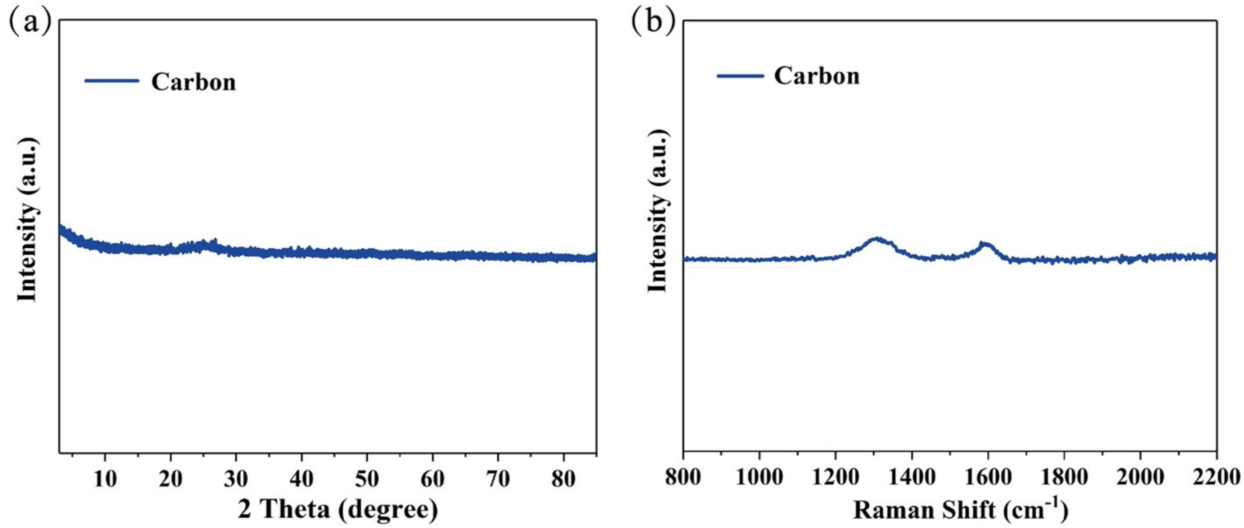

Fig. S12. (a) XRD pattern of carbon (etching NiO and Ni of C@NiO@Ni by HNO_3). (b) Raman pattern of carbon (etching NiO and Ni of C@NiO@Ni by HNO_3).

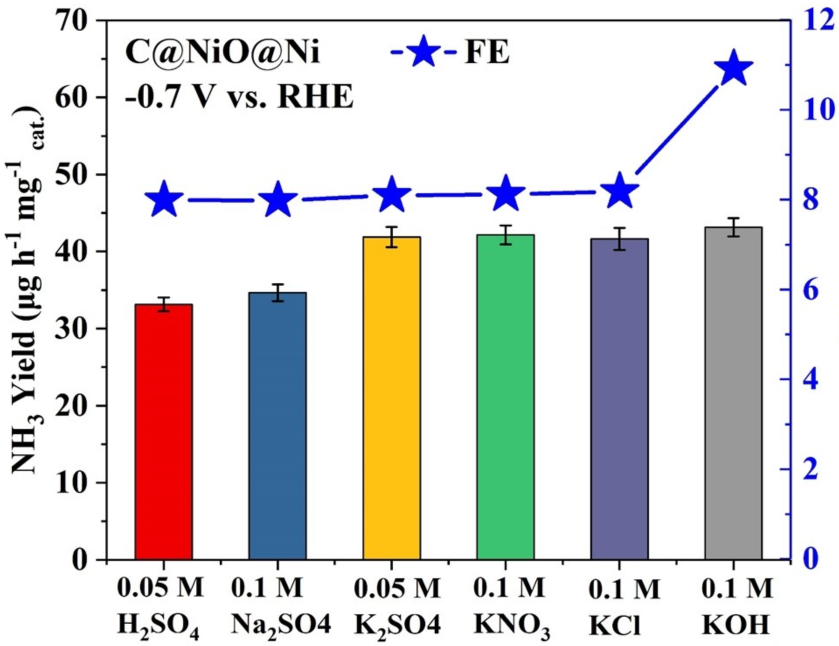

Fig. S13. NRR performance of C@NiO@Ni in different electrolytes at -0.7 V.

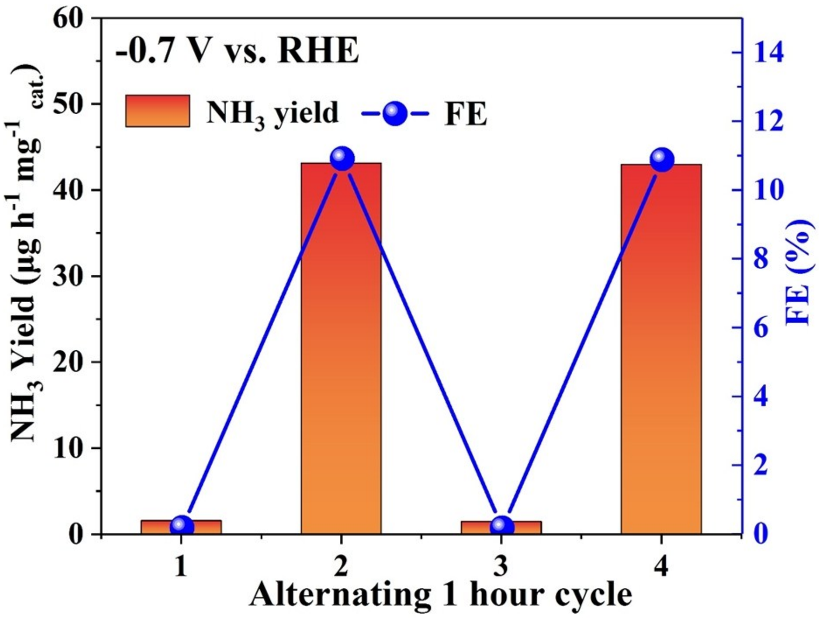

Fig. S14. NH_3 yields and FEs of C@NiO@Ni with alternating 1 h cycles between Ar atmosphere and N_2 atmosphere, for a total of 4 hours.

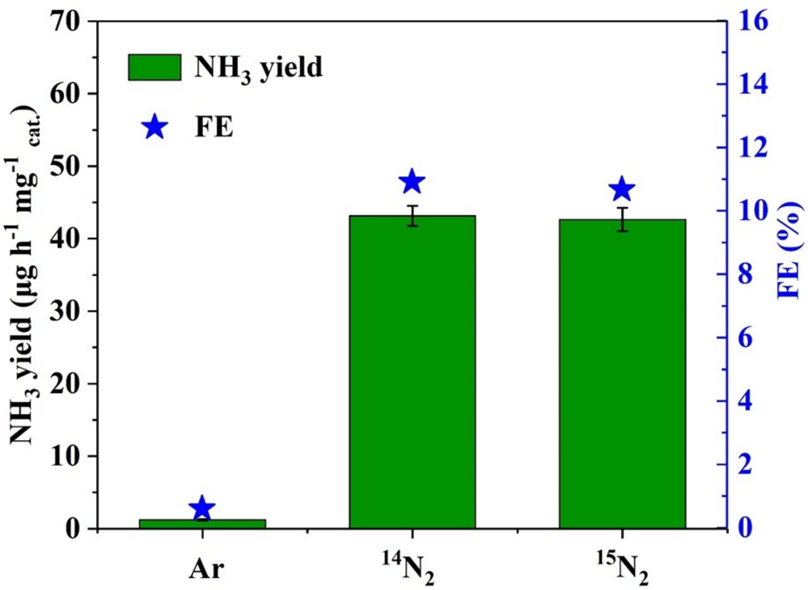

Fig. S15. Comparison of the Faradaic efficiency and NH_3 yield of C@NiO@Ni using different feeding gases for the NRR at -0.7 V.

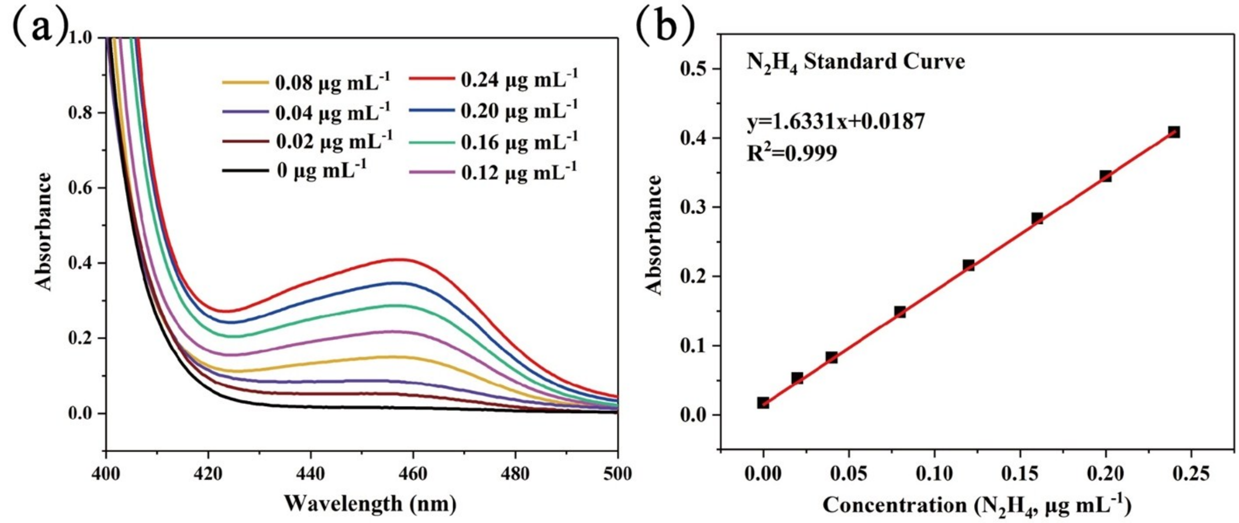

Fig. S16. (a) UV-Vis curves of various concentrations of N_2H_4 stained with p-$C_9H_{11}NO$ indicator. (b) A calibration curve used to estimate the concentrations of N_2H_4.

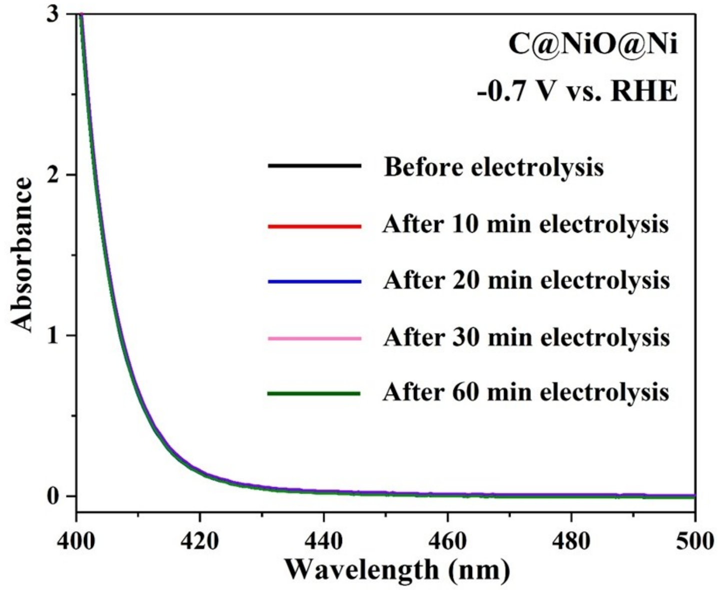

Fig. S17. UV-Vis absorption spectra of the electrolytes stained with p-$C_9H_{11}NO$ indicator after NRR electrolysis at different time.

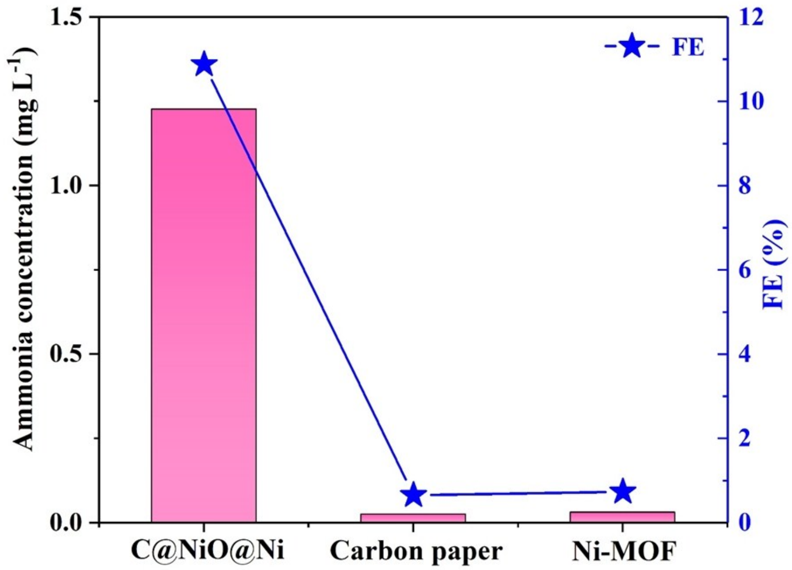

Fig. S18. Ammonia concentration and FE of C@NiO@Ni/CP, Ni-MOF/CP and CP after 1 h electrolysis at a potential of –0.7 V under ambient conditions.

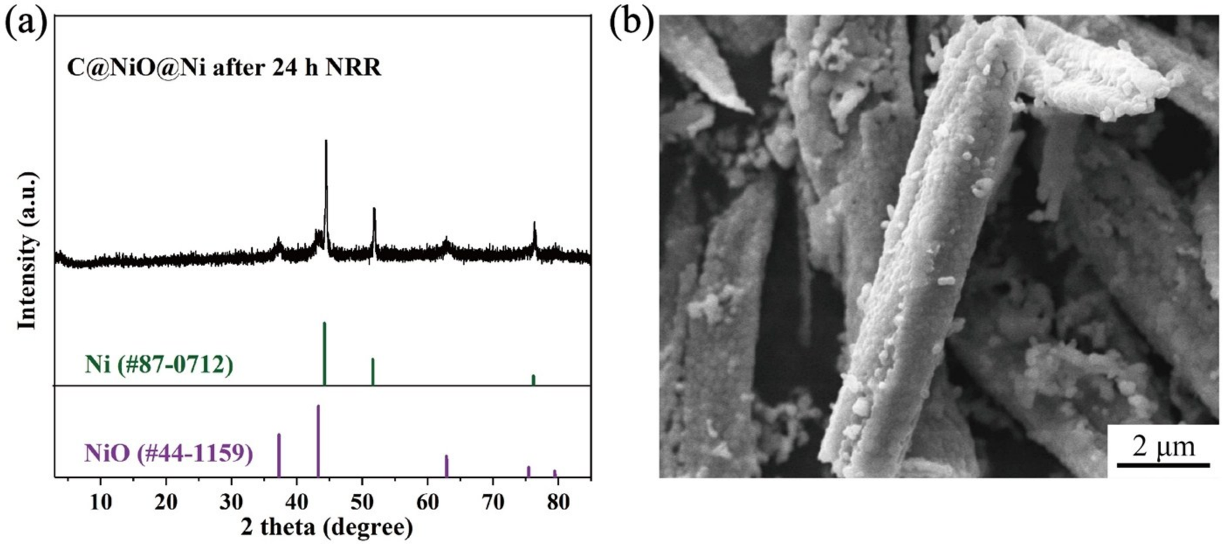

Fig. S19. (a) XRD pattern, (b) SEM image of C@NiO@Ni after 24 h NRR.

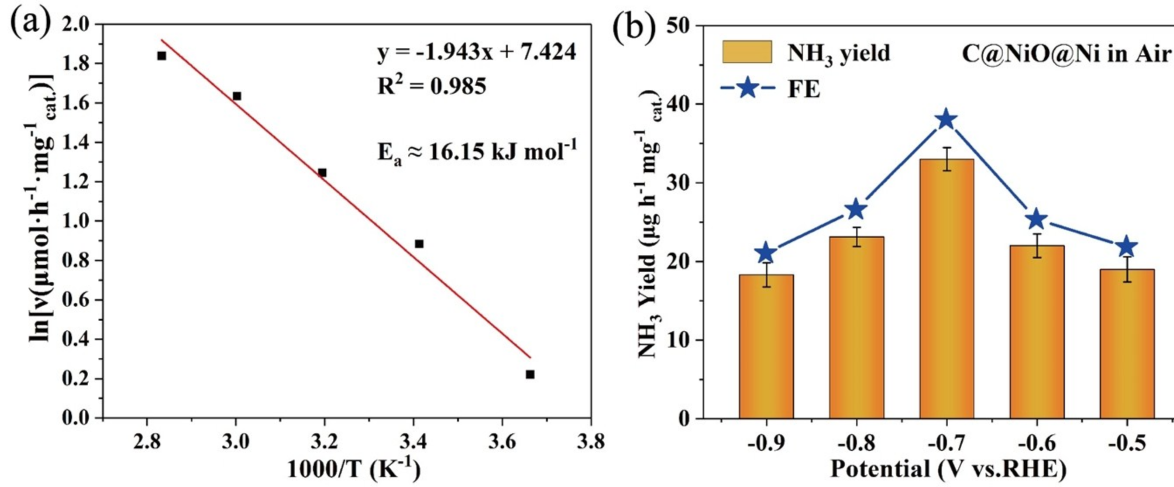

Fig. S20. (a) Arrhenius plot of the NRR rate over C@NiO@Ni catalyst at the temperature from 273 to 353 K. (b) NH_3 yields and FE for C@NiO@Ni at different potentials in Air.

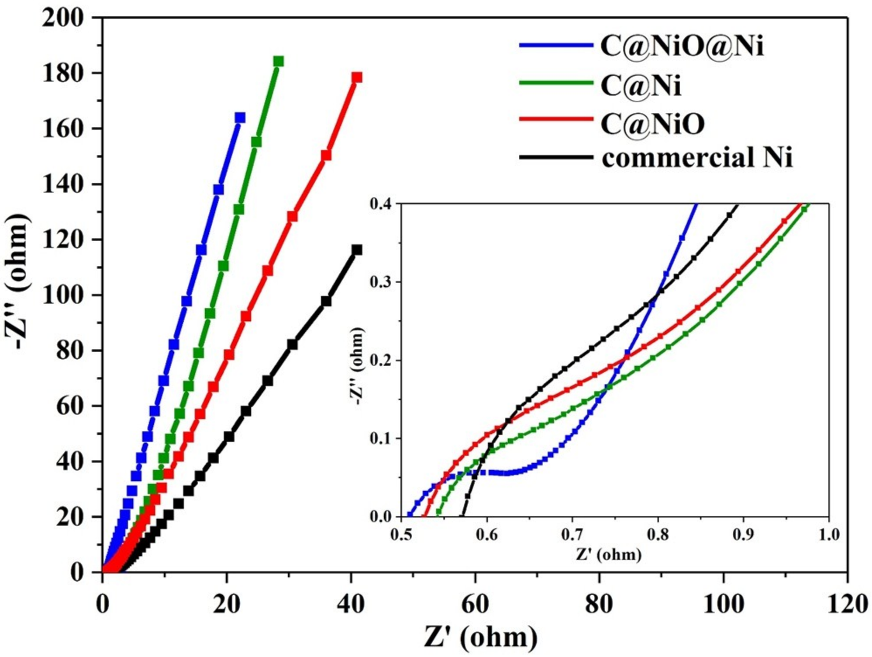

Fig. S21. EIS plots of C@Ni, C@NiO@Ni, C@Ni and commercial Ni in 0.1 M KOH.

Table S1. Comparison of the electrocatalytic activity of C@NiO@Ni to produce NH_3 through NRR with respect to the performances of other previously reported NRR electrocatalysts.

Catalyst	Electrolyte	NH_3 yield	FE (%)	Ref
C@NiO@Ni	**0.1 M KOH**	**43.15 μg h^{-1} $mg^{-1}_{cat.}$**	**10.9**	**This work**
Cr-doped CeO_2	0.1 M Na_2SO_4	16.82μg h^{-1} mg^{-1}	3.84	1
Bi_2MoO_6	0.1 M HCl	20.46 μg h^{-1} $mg^{-1}_{cat.}$	8.17	2
Co_3O_4@NC	0.05M H_2SO_4	42.58 μg h^{-1} $mg^{-1}_{cat.}$	8.49	3
Fe_2O_3-CNT	$KHCO_3$	0.22 μg h^{-1} cm^{-2}	0.15	4
TA-reduced Au/TiO_2	0.1 M HCl	21.4 μg h^{-1} $mg^{-1}_{cat.}$	8.11	5
Au nanorods	0.1 M KOH	1.6 μg h^{-1} cm^{-2}	3.88	6
α-Au/CeO_x-RGO	0.1 M HCl	8.31 μg h^{-1} $mg^{-1}_{cat.}$	10.1	7
Rh nanosheet nanoassemblies	0.1 M KOH	23.88 μg h^{-1} $mg^{-1}_{cat.}$	0.22	8
Pd/C	0.1 M PBS	4.5 μg h^{-1} mg^{-1}cat.	8.2	9
Ru/C	2 M KOH	0.21 μg h^{-1} cm^{-2}	0.28	10
AuHNCs	0.5 M $LiClO_4$	3.90 μg h^{-1} cm^{-2}	30.2	11
γ-Fe_2O_3 nanoparticles	0.1 M KOH	0.212 μg h^{-1} $mg^{-1}_{cat.}$	1.9	12
Fe_3O_4/Ti	0.1 M Na_2SO_4	5.6×10^{-11} mol s^{-1} cm^{-2}	2.6	13
N-doped porous carbon	0.05 M H_2SO_4	23.8 μg h^{-1} $mg^{-1}_{cat.}$	1.42	14
PCN-NV4	0.1 M HCl	8.09 μg h^{-1} $mg^{-1}_{cat.}$	11.59	15
N-doped carbon nanospikes	0.25 M $LiClO_4$	97.18 μg h^{-1} cm^{-2}	11.56	16
$Bi_4V_2O_{11}$/CeO_2	0.1 M HCl	23.21 μg h^{-1} $mg^{-1}_{cat.}$	10.16	17

Mo nanofilm	0.01 M H_2SO_4	1.89 μg h^{-1} cm^{-2}	0.72	18
MoS_2/CC	0.1 M Na_2SO_4	4.94 μg h^{-1} cm^{-2}	1.17	19
MoO_3	0.1 M HCl	29.43μg h^{-1} $mg^{-1}_{cat.}$	1.9	20
Mo_2N	0.1 M HCl	78.4 μg h^{-1} $mg^{-1}_{cat.}$	4.5	21
MoN	0.1 M HCl	3.01×10^{-10} mol s^{-1} cm^{-2}	1.15	22
Nb_2O_5 nanofiber	0.1 M HCl	43. 5 μg h^{-1} $mg^{-1}_{cat.}$	9.26	23
hollow Cr_2O_3 microspheres	0.1 M Na_2SO_4	25. 3 μg h^{-1} $mg^{-1}_{cat.}$	6.78	24
Mn_3O_4	0.1 M Na_2SO_4	11. 6 μg h^{-1} $mg^{-1}_{cat.}$	3.0	25
MoS_2 Nanoflower	0.1 M Na_2SO_4	29. 3 μg h^{-1} $mg^{-1}_{cat.}$	8.34	26
SnO_2/CC	0.1 M Na_2SO_4	1.47×10^{-10} mol s^{-1} cm^{-2}	2.17	27
b-FeOOH nanorods	0.5 M $LiClO_4$	23. 3 μg h^{-1} $mg^{-1}_{cat.}$	6.7	28
TiO_2–rGO	0.1 M Na_2SO_4	15. 1 μg h^{-1} $mg^{-1}_{cat.}$	3.3	29
B_4C	0.1 M HCl	26. 6 μg h^{-1} $mg^{-1}_{cat.}$	16.0	30

References

1 H. Xie, H. Wang, Q. Geng, Z. Xing, W. Wang, J. Chen, L. Ji, L. Chang, Z. Wang and J. Mao, *Inorg. Chem.*, 2019, **58**, 5423-5427.

2 Z. Xing, W. Kong, T. Wu, H. Xie, T. Wang, Y. Luo, X. Shi, A. M. Asiri, Y. Zhang and X. Sun, *ACS Sustain. Chem. Eng.*, 2019, DOI: 10.1021/acssuschemeng.9b03141.

3 S. Luo, X. Li, B. Zhang, Z. Luo and M. Luo, *ACS Appl. Mater. Inter.*, 2019, **11**, 26891-26897.

4 S. Chen, S. Perathoner, C. Ampelli, C. Mebrahtu, D. Su and G. Centi, *Angew. Chem., Int. Ed.*, 2017, **129**, 2743-2747.

5 M. M. Shi, D. Bao, B. R. Wulan, Y. H. Li, Y. F. Zhang, J. M. Yan and Q. Jiang, *Adv. Mater.*, 2017, **29**, 1606500.

6 D. Bao, Q. Zhang, F.-L. Meng, H.-X. Zhong, M.-M. Shi, Y. Zhang, J.-M. Yan, Q. Jiang and X.-B. Zhang, *Adv. Mater.*, 2017, **29**, 1604799.

7 S.-J. Li, D. Bao, M.-M. Shi, B.-R. Wulan, J.-M. Yan and Q. Jiang, *Adv. Mater.*, 2017, **29**, 1700001.

8 X. Y. Cui, C. Tang, X. M. Liu, C. Wang, W. J. Ma and Q. Zhang, *Chem.-Eur. J.*, 2018, **24**, 18494-18501.

9 J. Wang, L. Yu, L. Hu, G. Chen, H. Xin and X. Feng, *Nat. Commun.*, 2018, **9**, 1795.

10 V. Kordali, G. Kyriacou and C. Lambrou, *Chem. Commun.*, 2000, **17**, 1673-1674.

11 M. Nazemi, S. R. Panikkanvalappil and M. A. El-Sayed, *Nano Energy*, 2018, **49**, 316-323.

12 J. Kong, A. Lim, C. Yoon, J. H. Jang, H. C. Ham, J. Han, S. Nam, D. Kim, Y.-E. Sung, J. Choi and H. S. Park, *ACS Sustain. Chem. Eng.*, 2017, **5**, 10986-10995.

13 Q. Liu, X. Zhang, B. Zhang, Y. Luo, G. Cui, F. Xie and X. Sun, *Nanoscale*, 2018, **10**, 14386-14389.

14 Y. Liu, Y. Su, X. Quan, X. Fan, S. Chen, H. Yu, H. Zhao, Y. Zhang and J. Zhao, *ACS Catal.*, 2018, **8**, 1186-1191.

15 C. Lv, Y. Qian, C. Yan, Y. Ding, Y. Liu, G. Chen and G. Yu, *Angew. Chem., Int. Ed.*, 2018, **57**, 10246-10250.

16 Y. Song, D. Johnson, R. Peng, D. K. Hensley, P. V. Bonnesen, L. Liang, J. Huang, F. Yang, F. Zhang, R. Qiao, A. P. Baddorf, T. J. Tschaplinski, N. L. Engle, M. C. Hatzell, Z. Wu, D. A. Cullen, H. M. Meyer, B. G. Sumpter and A. J. Rondinone, *Sci. Adv.*, 2018, **4**, e1700336.

17 C. Lv, C. Yan, G. Chen, Y. Ding, J. Sun, Y. Zhou and G. Yu, *Angew. Chem., Int. Ed.*, 2018, **57**, 6073-6076.

18 D. Yang, T. Chen and Z. Wang, *J. Mater. Chem. A*, 2017, **5**, 18967-18971.

19 L. Zhang, X. Ji, X. Ren, Y. Ma, X. Shi, Z. Tian, A. M. Asiri, L. Chen, B. Tang and X. Sun, *Adv. Mater.*, 2018, **30**, 1800191.

20 J. Han, X. Ji, X. Ren, G. Cui, L. Li, F. Xie, H. Wang, B. Li and X. Sun, *J. Mater. Chem. A*, 2018, **6**, 12974-12977.

21 X. Ren, G. Cui, L. Chen, F. Xie, Q. Wei, Z. Tian and X. Sun, *Chem. Commun.*, 2018, **54**, 8474-8477.

22 L. Zhang, X. Ji, X. Ren, Y. Luo, X. Shi, A. M. Asiri, B. Zheng and X. Sun, *ACS Sustain. Chem. Eng.*, 2018, **6**, 9550-9554.
23 J. Han, Z. Liu, Y. Ma, G. Cui, F. Xie, F. Wang, Y. Wu, S. Gao, Y. Xu and X. Sun, *Nano Energy*, 2018, **52**, 264-270.
24 Y. Zhang, W. Qiu, Y. Ma, Y. Luo, Z. Tian, G. Cui, F. Xie, L. Chen, T. Li and X. Sun, *ACS Catal.*, 2018, **8**, 8540-8544.
25 X. Wu, L. Xia, Y. Wang, W. Lu, Q. Liu, X. Shi and X. Sun, *Small*, 2018, **14**, e1803111.
26 X. Li, T. Li, Y. Ma, Q. Wei, W. Qiu, H. Guo, X. Shi, P. Zhang, A. M. Asiri, L. Chen, B. Tang and X. Sun, *Adv. Energy. Mater.*, 2018, **8**, 1801357.
27 L. Zhang, X. Ren, Y. Luo, X. Shi, A. M. Asiri, T. Li and X. Sun, *Chem. Commun.*, 2018, **54**, 12966-12969.
28 X. Zhu, Z. Liu, Q. Liu, Y. Luo, X. Shi, A. M. Asiri, Y. Wu and X. Sun, *Chem. Commun.*, 2018, **54**, 11332-11335.
29 X. Zhang, Q. Liu, X. Shi, A. M. Asiri, Y. Luo, X. Sun and T. Li, *J. Mater. Chem. A*, 2018, **6**, 17303-17306.
30 W. Qiu, X. Y. Xie, J. Qiu, W. H. Fang, R. Liang, X. Ren, X. Ji, G. Cui, A. M. Asiri, G. Cui, B. Tang and X. Sun, *Nat. Commun.*, 2018, **9**, 3485.